VLTI's view on the circumstellar environment of cool evolved stars

K. Ohnaka

Max-Planck-Institut für Radioastronomie
Auf dem Hügel 69, D-53121 Bonn, Germany

Abstract

Infrared spectro-interferometry provides us with a unique opportunity to study the circumstellar environment of cool evolved stars in great detail, with spectral and spatial information disentangled. Recently, ESO's Very Large Telescope Interferometer (VLTI) has shed new light on the molecule and dust formation close to the photosphere or the structure of circumstellar disks around cool evolved stars. Our VLTI/MIDI observations of the oxygen-rich Mira star RR Sco have revealed the wavelength dependence of the angular size of the Mira star from 8 to 13 μm, which can be well explained by the presence of extended and dense H_2O layers and an optically thin dust shell. On the other hand, our MIDI observations of the silicate carbon star IRAS08002-3803 indicate the presence of an optically thick circumbinary disk, but the dust chemistry in the disk has turned out to be more complicated than previously thought. These results demonstrate the power of spectro-interferometry for obtaining new insights into the circumstellar environment of cool evolved stars.

Key words: interferometry, infrared, AGB and post-AGB, mass loss, circumstellar matter

1 Introduction

At the late stage of stellar evolution, stars return most of their mass to the interstellar space via mass loss before they end their life in supernova explosions in the case of massive stars ($M \gtrsim 8\ M_{\odot}$) or as planetary nebulae (PNe) in the case of low- and intermediate-mass stars. While mass loss plays an important role not only in stellar evolution but also in the chemical evolution of the Galaxy, the mass loss mechanism of (hot and cool) evolved stars is

Email address: kohnaka@mpifr-bonn.mpg.de (K. Ohnaka).

still little understood. In the circumstellar environment of cool evolved stars such as asymptotic giant branch (AGB) stars or red supergiants (RSGs), complicated physical and chemical processes take place, being mutually coupled: stellar pulsation, molecule and dust formation, chromospheric heating, and acceleration of mass outflows. For a better understanding of the mass loss mechanism in cool evolved stars, it is essential to obtain information on the physical properties of the region between the photosphere and the expanding dust shell—exactly the region where mass outflows are expected to be initiated. Another puzzling aspect of the mass loss phenomenon in cool evolved stars is the morphological evolution of the circumstellar envelope. Circumstellar envelopes around stars still at the AGB mostly show overall spherical symmetry, particularly on a large spatial scale (e.g., Izumiura et al., 1996; Neri et al. , 1998; Olofsson et al., 2000; González Delgado et al., 2003). However, objects at the very late stage of the AGB and their descendants—post-AGB stars, proto-planetary nebulae (PPNe), and PNe—show complicated structures such as clumps, disks, striking axisymmetric features, or even more complex morphology (e.g., Sahai & Trauger, 1998; Hofmann et al., 2001; Tuthill et al., 2002; Weigelt et al., 2002). However, it is by no means clear how and when these deviations from spherical symmetry occur or how such disks form. Obviously, high-spatial resolution observations, particularly when combined with spectroscopy (i.e., *spectro-interferometry*), provide us with a unique opportunity to address these problems. In the present paper, we show two examples of spectro-interferometric studies on cool evolved stars using the MID-infrared Interferometric instrument (MIDI) at the VLTI.

2 MIDI observation of the Mira star RR Sco

Recent spectroscopic and interferometric observations have revealed the presence of quasi-static, dense "warm molecular layers" in AGB stars, which are extending to a few stellar radii and characterized by temperatures of 1000–2000 K (Tsuji et al., 1997; Perrin et al., 2004; Ohnaka et al., 2004, and references therein). These molecular layers are located between the top of the photosphere and the expanding dust shell, and therefore, are most likely to play an important role in driving mass outflows.

We observed the oxygen-rich Mira star RR Sco with VLTI/MIDI in order to probe the physical properties of these warm molecular layers and the dust formation zone. The observations were carried out on 2003 June 14, 15, and 16 (RR Sco's variability phase = 0.6, minimum light) using the UT1-UT3-102m baseline in the prism mode ($\lambda/\Delta\lambda \approx 30$). Figure 1a shows the observed N-band visibilities as a function of wavelength. As shown in the figure, the projected baseline lengths range from 74 to 102 m. In order to derive the representative angular size in the N band, we fitted the observed visibility

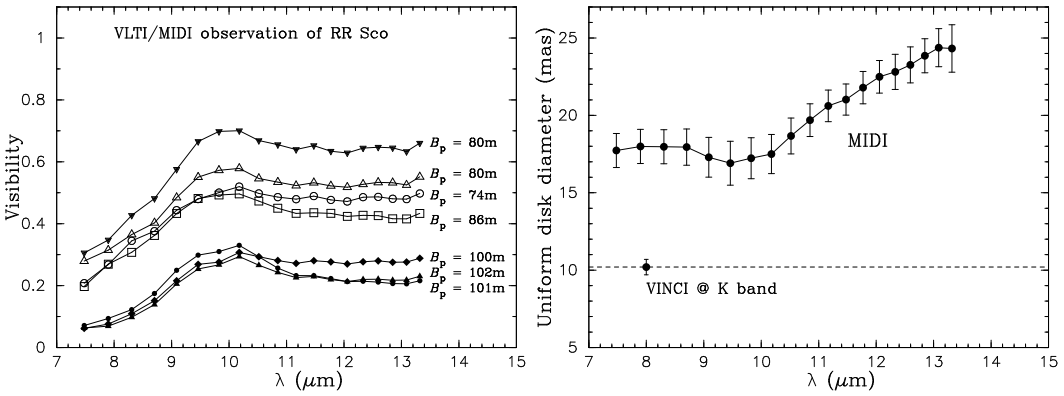

Fig. 1. *Left:* The observed N-band visibilities of RR Sco. All curves show a similar shape: a gradually increasing part shortward of 10 μm and a roughly constant part longward of 10 μm. The errors of the calibrated visibilities are typically 10–15%, but the error bars are omitted for the sake of clarity. *Right:* Uniform-disk diameter as a function of wavelength. The K-band uniform-disk diameter measured with VINCI is also plotted.

points at each wavelength with a uniform-disk, and the uniform-disk diameters obtained in this manner are plotted in Fig. 1b. The derived uniform-disk diameters are characterized by roughly a constant part between 8 and 10 μm (18 mas) and a gradual increase longward of 10 μm to reach $\sim$25 mas at 13 μm. In addition to the MIDI measurements, we used K-band VLTI/VINCI observations of RR Sco which are publicly available in the ESO archive. These VINCI observations were carried out on 2003 July 10 and 11, roughly three weeks after the MIDI observations. The two VLTI siderostats on stations E0 and G0 were used with a baseline length of 16 m. We fitted the observed visibility points with a uniform disk, and the resulting K-band uniform-disk diameter of 10.2 ± 0.5 mas is significantly smaller than the N-band diameters derived with MIDI (see Fig. 1b). It should be stressed, however, that we use uniform-disk fits to obtain some kind of representative angular size of the object and that it can be misleading to deduce quantitatively the nature of the object's intensity distribution based on such uniform-disk fits. In fact, as shown below, we compare models with the observed visibilities, not uniform-disk diameters, for the interpretation of the MIDI and VINCI data.

We attempt to interpret the observed visibility using a simple model of the warm molecular envelope and an optically thin dust shell. In this semi-empirical model, the star is surrounded by a warm molecular envelope consisting of H_2O and SiO gas with a constant temperature and density, and the inner radius of the molecular envelope is set to be equal to the stellar radius ($R_\star$). With this simplification, the intensity contribution of the star (approximated with the blackbody of $T_{\rm eff}$) and the molecular layer at a given distance from the stellar center r (i.e., a given line of sight) is obtained by $B_\lambda(T_{\rm mol})(1 - {\rm e}^{-\tau_\lambda}) + B_\lambda(T_{\rm eff}){\rm e}^{-\tau_\lambda}{\rm circ}(r/R_\star)$, where $T_{\rm mol}$ is the temperature of the molecular layer, ${\rm circ}(r/R_\star)$ takes a value of 1 for $r < R_\star$ and 0 elsewhere, and τ_λ is

the monochromatic optical depth of the layer along the given line of sight, which is computed from detailed line lists of H_2O transitions. We also add the contribution of an optically thin dust shell consisting of a mixture of silicate and corundum (Al_2O_3) to the warm H_2O+SiO envelope model, and the intensity profile and the total flux are computed. The monochromatic visibility squared is calculated by taking the Hankel transform of the model intensity. The calculated monochromatic visibility squared is then spectrally convolved to match the MIDI's spectral resolution of 30. The details of the modeling are described in Ohnaka et al. (2005).

We search for a best-fit model using the observed N-band (MIDI) and K-band (VINCI) visibilities as well as the N-band spectrum as observational constraints. Figure 2 shows a comparison of the observed visibility, uniform-disk diameter, and spectrum with those predicted by the best-fit model. In this model, the H_2O+SiO envelope is extending to 2.3 ± 0.2 $R_\star$ with a temperature of 1400 ± 100 K, and the H_2O and SiO column densities are 3×10^{21} and 1×10^{20} cm^{-2}, respectively. The optical depth of the dust shell is derived to be 0.025 ± 0.01 at 10 μm, which translates into 0.23 in the visible. The dust shell has an inner boundary radius of 7.5 $R_\star$ (dust temperature 700 K) and consists of 20% silicate and 80% corundum. The model uniform-disk diameter shown in Fig. 2 is derived by fitting the model visibility predicted for a baseline length of 100 m with a uniform-disk at each wavelength. Between 8 and 10 μm, optically thick emission from H_2O and SiO gas makes the angular size roughly twice as large as the K-band diameter, which is close to the stellar continuum diameter. The contribution of the optically thin dust shell becomes more significant longward of 10 μm, leading to the gradual increase of the angular diameter. We note that the observed N-band spectra—MIDI spectrum and IRAS Low Resolution Spectrum (LRS)—do not show the prominent silicate feature centered at 10 μm but appear rather featureless. In fact, our model suggests that the dust shell is dominated by corundum, which exhibits a very broad feature between $\sim$10 and 20 μm, with only a minor contribution of silicate (a slight difference between the MIDI spectrum and IRAS LRS can be due to a temporal variation of the properties of the dust shell).

3 MIDI observation of the silicate carbon star IRAS08002-3803

As outlined in Sect. 1, mass loss at the AGB leads to the formation of circumstellar dust shells. Dust species formed in the circumstellar envelope reflect the photospheric chemical composition: oxygen-bearing dust such as silicate and corundum is observed around oxygen-rich stars (M giants), while amorphous carbon or SiC are observed around carbon stars. Therefore, carbon stars showing circumstellar silicate emission discovered in the IRAS LRS (Little-Marenin, 1986; Willems & de Jong, 1986) struck stellar spectroscopists as

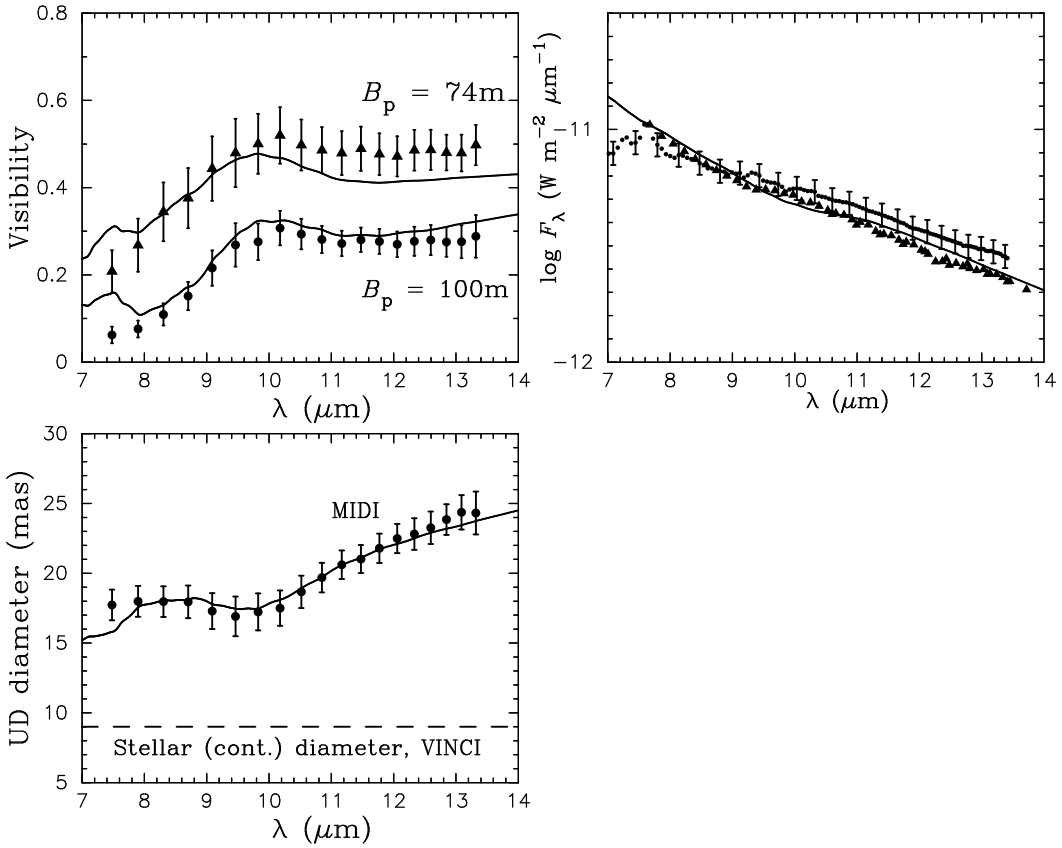

Fig. 2. *Upper left*: Filled circles and triangles: the visibilities observed with projected baseline lengths of 99.9 m and 73.7 m, respectively. Solid lines: the corresponding model visibilities. *Lower left*: Filled circles: the observed uniform-disk diameters. Solid line: the model uniform-disk diameter derived for the 100 m baseline. Dashed line: the continuum stellar angular diameter estimated from the VINCI observations. *Upper right*: Filled circles: the calibrated MIDI spectrum of RR Sco. Filled triangles: IRAS LRS. Solid line: the spectrum predicted by the model.

baffling. Willems & de Jong (1986) and Chan & Kwok (1988) suggested that silicate carbon stars are objects in transition from O-rich M giants to carbon stars, while Little-Marenin (1986) suggested that they are binaries consisting of a carbon star and an M giant. However, these scenarios are now rejected on various observational grounds (e.g., Ohnaka et al., 2006, and references therein). The widely believed hypothesis suggests that silicate carbon stars have a low-luminosity companion (a main-sequence star or a white dwarf) and that O-rich material was shed by mass loss when the primary star was an M giant and this O-rich material is stored in a circumbinary disk or in a circum-companion disk until the primary star becomes a carbon star (Morris, 1987; Lloyd-Evans, 1990; Yamamura et al., 2000). However, these binary scenarios have been neither observationally nor theoretically confirmed, and the origin of silicate carbon stars is still a puzzle to date. Observations with high spatial resolution within the silicate emission feature at 10 μm would be a most direct approach for investigating the dusty environment of silicate

carbon stars.

IRAS08002-3803 was observed with MIDI on 2004 February 9, 10, and 11 in the prism mode ($\lambda/\Delta\lambda \simeq 30$) using the UT2-UT3-47m baseline. Details of our MIDI observations and data reduction as well as the modeling discussed below are given in Ohnaka et al. (2006). Figure 3a shows the observed N-band visibilities of IRAS08002-3803. The figure reveals that all visibilities derived from four data sets show a distinct wavelength dependence: a steady increase from 8 to $\sim$10 μm and a nearly constant part longward of 10 μm with a very slight decrease. This wavelength dependence of the observed visibility translates into roughly constant uniform-disk diameters between 8 and 10 μm and a rather steep increase longward of 10 μm, as shown in Fig. 3c. Such a wavelength dependence of the angular size in the N band is rather unexpected. The angular size of an object with prominent silicate emission (see Fig. 3b) is expected to be larger at 10 μm than at 8 μm, because the contribution of the extended silicate emission is higher at 10 μm, and the stellar contribution also becomes smaller from 8 to 10 μm. In fact, we attempted to explain the observed spectral energy distribution (SED) of IRAS08002-3803 and the N-band visibilities with spherical shells or axisymmetric disk models containing silicate dust by using a Monte Carlo radiative transfer code. However, while such models can reproduce the observed SED quite well, they fail to reproduce the observed wavelength dependence of the N-band visibilities. That is, the visibilities predicted by these models decrease from 8 to 10 μm and increase slowly or slightly longward of 10 μm, in clear disagreement with the MIDI observations (see Fig. 4c). In fact, we could not find a parameter set which can simultaneously reproduce the SED and N-band visibilities in the disk (and shell) geometry consisting of silicate dust alone.

As a possible scenario to explain the observed SED and N-band visibilities, we consider models with two grain species, (amorphous) silicate and some other grain species. Since the IRAS LRS and MIDI spectrum do not show prominent features other than the broad 10 μm feature, we tentatively consider the following three grain species, which exhibit no conspicuous spectral features in the wavelength range covered by these spectra: amorphous carbon, large silicate grains, and metallic iron grains. It has turned out that the disk models with amorphous silicate and these second grain species can fairly – though not entirely satisfactorily – reproduce the observed SED and N-band visibilities simultaneously. As an example, we show the best-fit disk model with silicate and metallic iron in Fig. 4. In this model, the optical depths of silicate and iron dust are found to be 20 ± 5 and 3 ± 1 at 0.55 μm, respectively, which correspond to 10 μm optical depths of 1.5 and 0.34, respectively. The disk has a half-opening angle of $50^\circ \pm 10^\circ$ and an inner boundary radius of 20 ± 5 $R_\star$, where the temperatures of silicate and iron grains reach $\sim$620 K, with density proportional to $r^{-1.6\pm0.1}$. The inclination angle is derived to be $30^\circ \pm 10^\circ$. Figure 4a shows that the observed SED is fairly reproduced by the model,

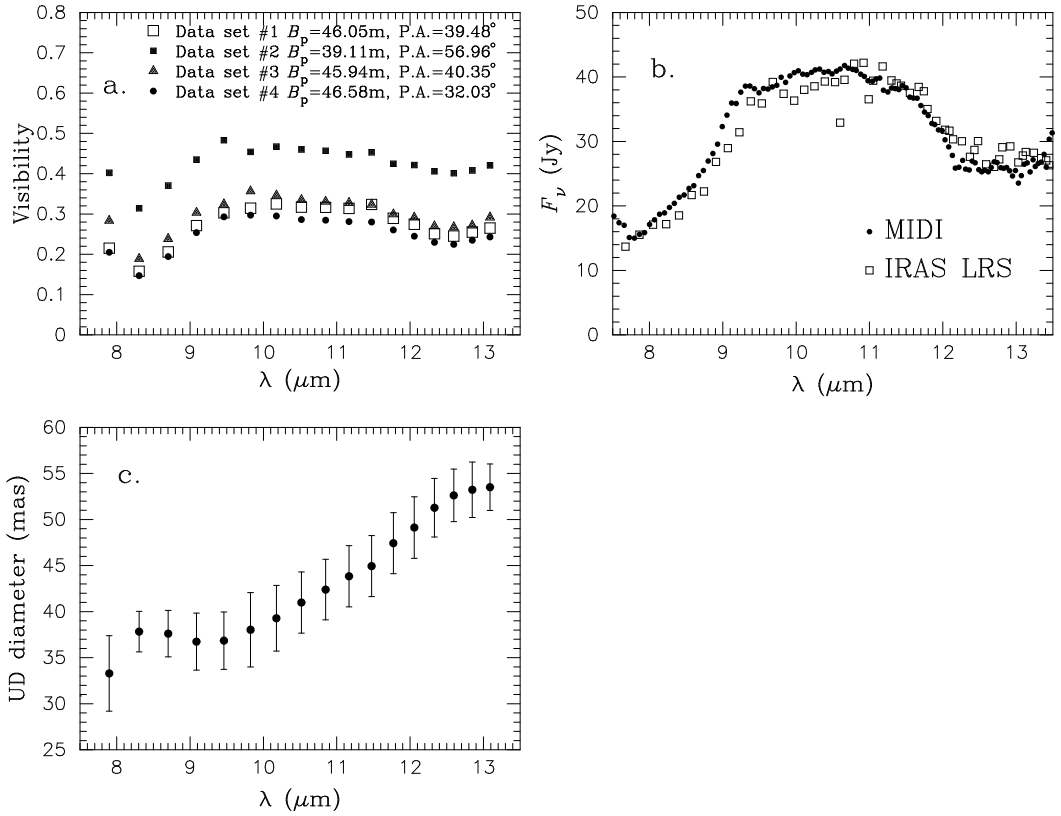

Fig. 3. **a**: The N-band visibilities of IRAS08002-3803 observed with MIDI. **b**: N-band spectra observed with MIDI and IRAS LRS. **c**: The uniform-disk diameters derived by fitting the observed visibilities.

although the model predicts the near-infrared flux to be slightly lower than the observations. Figure 4c reveals that the wavelength dependence of the N-band visibilities predicted by this model is also in fair agreement with the MIDI observations. The intensity distributions of the silicate and metallic iron components show different wavelength dependences, and the flux contributions of these two components also vary in the N band. Since the total visibility is the flux-weighted sum of two visibility components, the combination of these factors results in a wavelength dependence of the N-band visibility totally different from that predicted by the models with silicate dust alone.

However, there are still discrepancies between the observations and the models. The predicted visibilities are somewhat too flat between 8 and 10 μm compared to those observed, which is also the case for the models containing amorphous carbon or large silicate grains as the second grain species. This discrepancy may be attributed to the assumptions used in our models, such as the rather simplified disk geometry and representation of the dust properties. An alternative explanation would be to assume that different grain species have different spatial distributions, instead of coexisting everywhere in the disk. It is plausible that distinct regions of the disk may be predominantly populated with different grain species due to the grain formation and growth

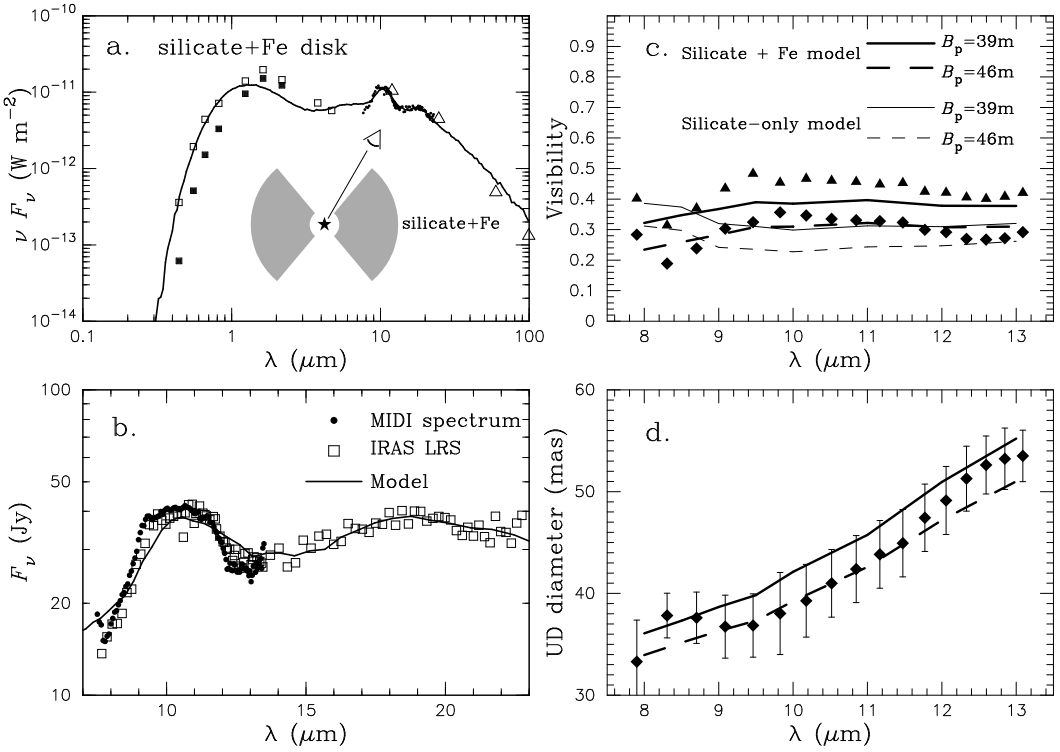

Fig. 4. Circumbinary disk model of IRAS08002-3803 consisting of silicate and metallic iron from Ohnaka et al. (2006). The disk is optically thick with 0.55 μm optical depths of 20 and 3 for silicate and iron grains, respectively, and has an inner radius of 20 $R_\star$ ($\sim$40 AU). **a.** Open and filled squares: observed SED (corrected and not corrected for interstellar extinction). Open triangles: IRAS fluxes. Dots: IRAS LRS. Solid line: model SED. The viewing angle is depicted in the inset. **b.** Comparison of SEDs in the mid-infrared region. **c.** Filled triangles and diamonds: N-band visibilities observed with 39 m and 46 m baselines, respectively. Thick solid and dashed lines: the corresponding model visibilities predicted by the silicate+Fe model. The visibilities predicted by a silicate-only disk model are also plotted by the thin solid and dashed lines for comparison. **d.** Filled diamonds: the observed uniform disk diameters. Solid and dashed lines: model uniform-disk diameters for 39 m and 46 m baselines.

processes. However, more complementary observational constraints would be needed to explore such spatial variations of dust chemistry.

4 Concluding remarks

The two studies based on VLTI/MIDI observations shown above demonstrate that spectro-interferometry is a powerful tool for studying the circumstellar environment of cool evolved stars in detail. Our observations of the Mira star RR Sco show that the extended warm water vapor envelope, whose presence was first discovered by spectroscopy, makes the object appear remarkably

larger in the N band than in the K band, because the extended water vapor emission is significant in the former band than in the latter. The extended emission from the dust shell makes the object appear even larger longward of $\sim$10 μm. We have shown that the measurement of the wavelength dependence of the angular size over molecular as well as dust spectral features in the mid-infrared provides direct information on the geometrical extent of the warm molecular envelope, and such information, combined with spectral data, can help to put more constraints on physical properties of the warm molecular envelope.

On the other hand, our VLTI/MIDI observations of the silicate carbon star IRAS08002-3803 have revealed an unexpected wavelength dependence of the N-band visibility, which cannot be explained by spherical shells or disks consisting of silicate dust alone. Our radiative transfer modeling shows that the observed visibility and SED can be fairly explained by an optically thick disk consisting of silicate and a second grain species—amorphous carbon, large silicate grains, or metallic iron dust. This illustrates the power of spectro-interferometry to obtain entirely new insights into the circumstellar environment of cool evolved stars, which is not possible with spectroscopic data alone.

Still, there are a number of problems which have not yet been addressed. For example, the evolution of dust chemistry in the circumstellar shell or disk not only in AGB stars but also in post-AGB stars can be investigated by taking advantage of the high-angular resolution and spectroscopic capability of VLTI/MIDI (e.g., Deroo et al., 2006). Furthermore, the mechanisms responsible for the formation of asymmetries mentioned in Sect. 1 can be studied by VLTI observations covering different position angles (e.g., Chesneau et al., 2006). Also, studies on temporal variations of the outer atmosphere and the dust shell of AGB stars would be crucial for unraveling the driving mechanism of mass outflows. Thus, VLTI is expected to bring about more clues to the long-standing problems of cool evolved stars—and more intriguing new questions.

References

Chan, S.J., & Kwok, S., 1988, ApJ, 334, 362

Chesneau, O., Collioud, A., De Marco, O., et al., 2006, A&A, 455, 1009

Deroo, P., Van Winckel, H., Min, M., et al., 2006, A&A, 450, 181

González Delgado, D., Olofsson, H., Schwarz, H. E., et al., 2003, A&A, 399, 1021

Hofmann, K.-H., Balega, Y., Blöcker, T., & Weigelt, G., 2001, A&A, 379, 529

Izumiura, H., Hashimoto, O., Kawara, K., Yamamura, I., & Waters, L.B.F.M., 1996, A&A, 315, L221

Little-Marenin, I.R., 1986, ApJ, 307, L15

Lloyd-Evans, T., 1990, MNRAS, 243, 336
Morris, M., 1987, PASP, 99, 1115
Neri, R., Kahane, C., Lucas, R., Bujarrabal, V., & Loup, C., 1998, A&AS, 130, 1
Ohnaka, K., 2004, A&A, 424, 1011
Ohnaka, K., Bergeat, J., Driebe, T., et al., 2005, A&A, 429, 1057
Ohnaka, K., Driebe, T., Hofmann, K.-H., et al., 2006, A&A, 445, 1015
Olofsson, H., Bergman, P., Lucas, R., et al., 2000, A&A, 353, 583
Perrin, G., Ridgway, S.T., Mennesson, B., et al., 2004, A&A, 426, 279
Sahai, R., & Trauger, J., 1998, ApJ, 116, 1357
Tsuji, T., Ohnaka, K., Aoki, W., & Yamamura, I., 1997, A&A, 320, L1
Tuthill, P.G., Men'shchikov, A.B., Schertl, D., et al., 2002, A&A, 389, 889
Weigelt, G., Balega, Y.Y., Blöcker, T., et al., 2002, A&A, 392, 131
Willems, F., & de Jong, T., 1986, ApJ, 309, L39
Yamamura, I., Dominik, C., de Jong, T., Waters, L.B.F.M., & Molster, F.J., 2000, A&A, 363, 629